

RESEARCH ARTICLE

Ultraviolet filters in stomatopod crustaceans: diversity, ecology and evolution

Michael J. Bok^{*,§}, Megan L. Porter[‡] and Thomas W. Cronin

ABSTRACT

Stomatopod crustaceans employ unique ultraviolet (UV) optical filters in order to tune the spectral sensitivities of their UV-sensitive photoreceptors. In the stomatopod species *Neogonodactylus oerstedii*, we previously found four filter types, produced by five distinct mycosporine-like amino acid pigments in the crystalline cones of their specialized midband ommatidial facets. This UV-spectral tuning array produces receptors with at least six distinct spectral sensitivities, despite expressing only two visual pigments. Here, we present a broad survey of these UV filters across the stomatopod order, examining their spectral absorption properties in 21 species from seven families in four superfamilies. We found that UV filters are present in three of the four superfamilies, and evolutionary character reconstruction implies that at least one class of UV filter was present in the ancestor of all modern stomatopods. Additionally, postlarval stomatopods were observed to produce the UV filters simultaneously alongside development of the adult eye. The absorbance properties of the filters are consistent within a species; however, between species we found a great deal of diversity, both in the number of filters and in their spectral absorbance characteristics. This diversity correlates with the habitat depth ranges of these species, suggesting that species living in shallow, UV-rich environments may tune their UV spectral sensitivities more aggressively. We also found additional, previously unrecognized UV filter types in the crystalline cones of the peripheral eye regions of some species, indicating the possibility for even greater stomatopod visual complexity than previously thought.

KEY WORDS: Mantis shrimp, Ultraviolet vision, Optical filters, Mycosporine-like amino acids, Ancestral state reconstruction

INTRODUCTION

Stomatopod crustaceans, commonly referred to as mantis shrimp, are well known for charismatic, aggressive behavior (Caldwell and Dingle, 1975; Dingle and Caldwell, 1969) and their spectacularly elaborate visual systems (Cronin and Marshall, 1989a). Many species possess at least 16 spectral classes of photoreceptors in their retinas. Included in these are eight color-specialist photoreceptors sensitive to narrow ranges of ‘human-visible’ light (Cronin and Marshall, 1989a,b; Marshall, 1988), three polarization receptors sensitive to linearly or circularly polarized light (Chiou et al., 2008; Cronin et al., 1994b; Kleinlogel and Marshall, 2006; Marshall,

1988; Marshall et al., 1991a) and at least five receptors sensitive to various spectral ranges of ultraviolet (UV) light (Kleinlogel and Marshall, 2009; Marshall and Oberwinkler, 1999). Underlying these diverse visual sensitivities is an array of optical and retinal structural modifications (Horridge, 1978; Marshall et al., 1991a; Schiff et al., 1986), the expression of a great number of opsins resulting in the most visual pigments yet described in a single eye (Cronin and Marshall, 1989b; Cronin et al., 1993; Porter et al., 2009, 2013), and the tuning of spectral sensitivity via serial filtering effects due to more distal visual pigments as well as photostable colored pigments (Cronin and Marshall, 1989a; Cronin et al., 1994a,b, 2014; Marshall, 1988; Marshall et al., 1991b; Porter et al., 2010).

Stomatopod apposition compound eyes are subdivided into three regions. Most of the eye consists of the dorsal and ventral peripheral regions, which are bisected horizontally by a multi-row midband (Harling, 2000; Manning et al., 1984). The peripheral regions are composed of a homogeneous array of ommatidia presumably responsible for spatial vision. These ommatidia are organized similarly to those of other malacostracan crustaceans, with corneal and crystalline cone optical elements focusing light onto the retinal photoreceptors. Each ommatidium contains a proximal main rhabdom photoreceptor, produced by a cylindrical arrangement of reticular cells one to seven (R1–7), and a distal photoreceptor produced by reticular cell eight (R8). In stomatopods, R1–7 receptors in peripheral ommatidia are maximally sensitive to blue–green light, while the R8 is maximally sensitive to UV light. The notable diversification and specialization of stomatopod photoreceptors is found in the six midband rows of stomatopods from the superfamilies Gonodactyloidea, Lysiosquilloidea, Pseudosquilloidea and Hemisquilloidea (superfamilies as suggested in Porter et al., 2010). Here, the relatively simple ommatidial organization of the peripheral regions is modified into the most elaborate photoreceptor array in nature.

The R8 photoreceptors in the midband of gonodactyloids are responsible for the remarkable spectral diversity of the stomatopod UV visual system, with four distinct spectral classes (in addition to the single R8 spectral class in the periphery) having been identified by electrophysiology (Kleinlogel and Marshall, 2009; Marshall and Oberwinkler, 1999). In *Neogonodactylus oerstedii*, these R8s only contain two visual pigments, and the full spectral diversity is achieved by optical filtering effects from four distinct UV-specific filters located in the crystalline cones (Bok et al., 2014). The surprising localization of these filters in the crystalline cones was revealed by the fluorescent properties of three of the filter types found in rows 3–6, which emit blue, cyan or green light when stimulated with strong UV illumination. These filters are composed of mycosporine-like amino acids (MAAs), compounds commonly associated with photoprotection in marine organisms (Carreto and Carignan, 2011; Shick and Dunlap, 2002). In eukaryotes, MAAs are typically acquired through their diet (Hylander and Jephson, 2010;

Department of Biological Sciences, University of Maryland Baltimore County, 1000 Hilltop Circle, Baltimore, MD 21250, USA.

^{*}Present address: Department of Biology, Lund Vision Group, Lund University, Lund, Sweden. [‡]Present address: Department of Biology, University of Hawai‘i at Mānoa, Honolulu, HI 96822, USA.

[§]Author for correspondence (mikebok@gmail.com)

List of symbols and abbreviations

MAA	mycosporine-like amino acid
MSP	microspectrophotometry
R1–7	retinular cells 1–7, the main rhabdom
R8	retinular cell 8
UV	ultraviolet
UVF1–4	ultraviolet filters in crystalline cones, defined in Results
λ_{\max}	wavelength of maximum absorption

Newman et al., 2000) and subsequently modified for use as photoprotectants or, in the case of stomatopods, as optical filters.

Optical filters function by selectively absorbing and transmitting certain wavelengths of light, shaping the spectrum that reaches a photoreceptor, and thus altering its spectral sensitivity. Optical filtering is common in nature, with sets of multiple colored filters having been described in reptiles (Walls, 1942), birds (Goldsmith et al., 1984), lungfish (Bailes et al., 2006), butterflies (Arikawa and Stavenga, 1997; Arikawa et al., 1999a,b) and the main rhabdom photoreceptors of stomatopods (Cronin et al., 1994a; Marshall, 1988; Marshall et al., 1991b), among others (see Douglas and Marshall, 1999, for a review of optical filters in animals).

In *N. oerstedii*, five spectral classes of UV-specialist R8s are produced by the pairwise combination of only two visual pigments (wavelength of maximum absorption, λ_{\max} , at 334 and 383 nm, respectively), with four UV-specific optical filters in the crystalline cones (Bok et al., 2014). One type of UV filter, found in the crystalline cones of midband rows 1 and 2, is composed of the MAA porphyrin-334, with a λ_{\max} of 334 nm. Midband rows 3 and 4 express similar but distinct filter pigments, with λ_{\max} at 372 and 375 nm, respectively. These filters, which are responsible for the distinct fluorescent emission, do not match any currently characterized MAAs, and likely represent novel molecular structures. Finally, midband rows 5 and 6 contain identical notch filters composed of two pigments, mycosporine-glycine with a λ_{\max} of 308 nm and a second weaker optical density (OD) pigment with a λ_{\max} of 388 nm. This second pigment likely produces the green fluorescence visible in rows 5 and 6, and is also currently uncharacterized. The 334 nm visual pigment expressed in the R8s of midband rows 2 through to 6 is tuned to longer wavelengths by the pigments in the crystalline cones of rows 2, 5 and 6 (long-pass filtering), and to shorter wavelengths by the pigments of rows 3 and 4 (short-pass filtering).

Some stomatopod species can also have between two and four intrarhabdomal long-wavelength colored filters that act on the main rhabdom R1–7 photoreceptors in midband rows 2 and 3 (Cronin et al., 1994a; Marshall, 1988; Marshall et al., 1991b; Porter et al., 2010). Some species even tune the absorption properties of these filters by varying the lengths of the filters or altering the composition of the pigments they contain in order to best suit their spectral environment (Cheroske et al., 2006, 2003; Cronin and Caldwell, 2002; Cronin et al., 1994b, 2000, 2001). Considering the high degree of variability in the absorbance characteristics of these long-wavelength filters, we were curious to learn how the UV filters vary across species. Are these filters pervasive throughout the order, and can their physiological functions offer any clues to their evolution and ecological function? To these ends we set out to characterize the UV filters in a broad sampling of stomatopod taxa. We initially looked for UV-stimulated autofluorescence in the midband that belies the presence of certain UV filters. Of the 28 species we observed, only six lacked fluorophores in the midband, while the remainder displayed a beautiful diversity of fluorescent colors and patterns (Fig. 1). The presence and variability of these fluorophores from

species to species suggested that UV filters in stomatopods are physiologically complex and ecologically important.

Here, we present a spectral survey of the UV filters in 21 stomatopod species. We characterized the number, optical properties and variability of these filters, both within and between species. We used the most current phylogeny of the Stomatopoda to reconstruct the evolution of the UV filters, and we analyzed their ecological significance in species with differing habitats and lifestyles. Our examination of these UV filters suggests the presence of an even greater level of spectral diversification in stomatopod visual systems than earlier described, making the most spectrally elaborate eye in nature even more complex than previously thought.

RESULTS**Spectroscopy of UV filter pigments**

Using microspectrophotometry (MSP) and imaging spectrometry, we examined the crystalline cone absorbance spectra from 21 species of stomatopods representing seven families from all four superfamilies that have elaborated six-row midbands: Gonodactyloidea, Lysiosquilloidea, Pseudosquilloidea and Hemisquilloidea (Table 1, Fig. 2A). Also, the presence or absence of the fluorescent UV filters in seven additional species was determined by observation of UV-stimulated autofluorescence (supplementary material Table S1). Our survey indicated the presence of four primary filter UV types found in the midbands of stomatopods, each associated with particular rows of the midband. We refer to these filters as UVF1 (rows 1 and 2), UVF2 (row 3), UVF3 (row 4) and UVF4 (rows 5 and 6) (Fig. 2A, top left panel). Of the 21 species examined by MSP, 19 had at least one significant UV-absorbing pigment in the midband crystalline cones. Of these, eight had a single filter type, one had two filter types, two had three filter types, and eight had all four. The UVF3 filter is present in all 19 species that express any UV filters in the crystalline cones.

Spectral variability

The absorbance spectrum of each primary UV filter type was compared across all species. We found that there was significant variation among species (Fig. 2B), but within a species each filter type was fairly constrained spectrally, with the λ_{\max} rarely exceeding a standard deviation of ± 2 nm between individuals (Fig. 2C). The λ_{\max} of UVF1 varied by 10 nm among different species, UVF2 by 18 nm, UVF3 by 26 nm and UVF4 by at least 8 nm. For UVF1, filters of all but two species were very similar in shape, resembling the MAA porphyrin-334 previously identified in these rows in *N. oerstedii* (Bok et al., 2014). A similar case was found with UVF4, where most examples of this filter appear to be composed of mycosporine-glycine, with filters in only four species having a shorter wavelength absorbance spectrum. In UVF2 and UVF3 there was no single dominant spectral absorbance curve. These pigments instead have a fairly stereotypical shape that is shifted throughout the spectral range measured for each filter.

Evolution

The character state of the four primary UV filter types in stomatopods was reconstructed using the most recently published molecular phylogeny of the order (Porter et al., 2010, 2013), but including several additional species procured for this survey (supplementary material Table S2). This new tree agreed with the familial and superfamilial relationships reported in Porter et al. (2010). The number of UV filters found in each species based on the presence or absence of the four primary UV filter classes, UVF1–4, was used to

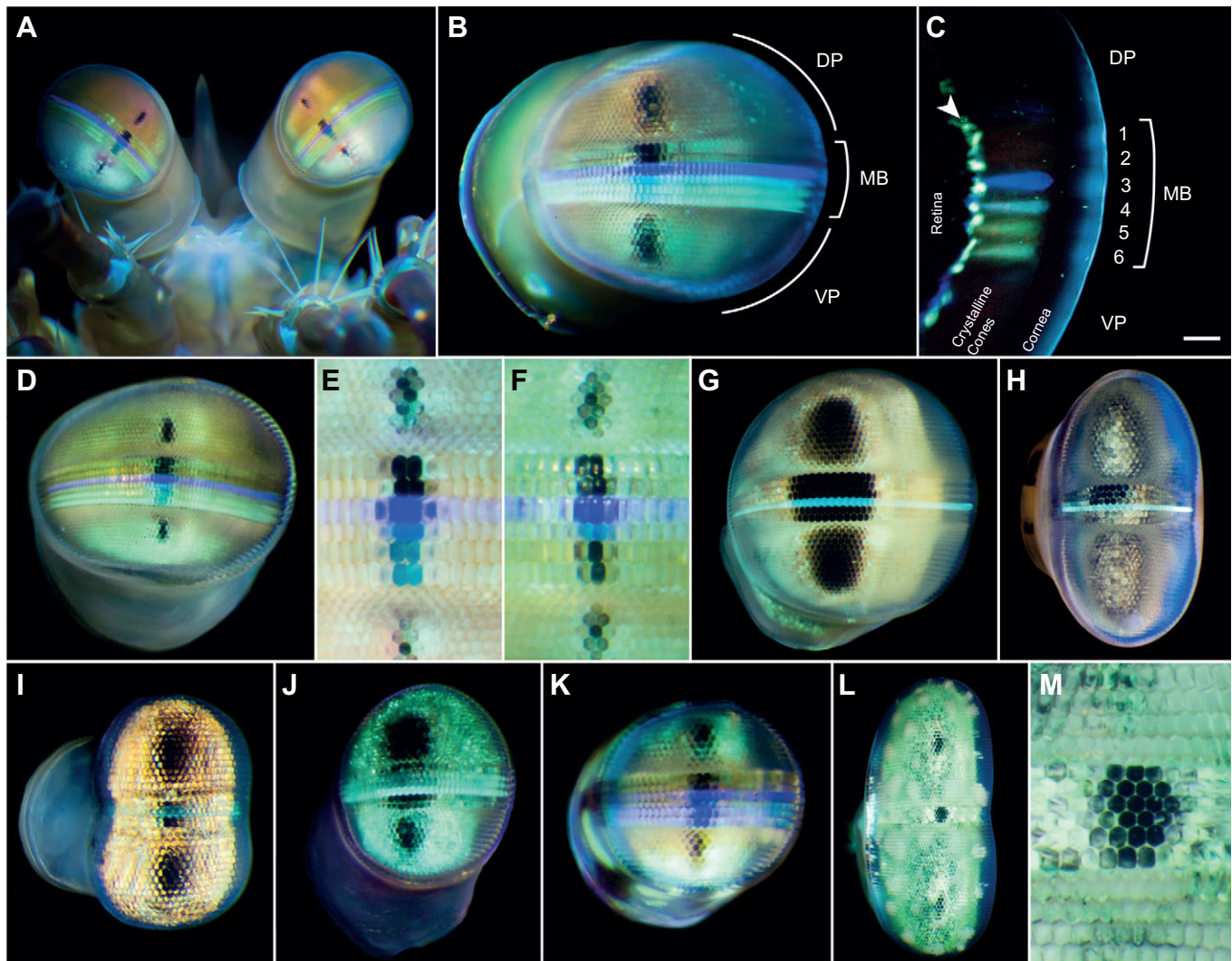


Fig. 1. UV-excited autofluorescence patterns in the eyes of various stomatopod species. Horizontal streaks of 375 nm light-stimulated autofluorescence indicative of UV filter pigments in the midband overlying the dark pseudopupil facets. Most other fluorescent emission outside the pseudopupil is an optically irrelevant distal pigment that overlays the retina outside the optical path. (A) The head of *Gonodactylus platysoma*. (B) The eye of *Gonodactylaceus falcatus* detailing the midband (MB), and dorsal and ventral peripheral regions (DP, VP). (C) A cross-section in the midband of *Neogonodactylus oerstedii* showing that the fluorophores are located in the crystalline cone optical layer. The distal pigment overlying the retina is indicated with an arrowhead. Scale bar, 100 μ m. (D) *Gonodactylus chiragra*. (E) *Neogonodactylus oerstedii* midband. (F) *Neogonodactylus wennekei* midband. (G) *Odontodactylus latirostris*. (H) *Pseudosquilla richeri*. (I) *Chorisquilla hystrix*. (J) *Haptosquilla glyptocercus*. (K) *Gonodactylellus affinis*. (L) *Lysiosquillina maculata*. (M) *Lysiosquillina maculata* midband enlarged, lacking UV fluorophores.

reconstruct the ancestral number of filters across the phylogeny (Fig. 3). The character state reconstruction indicated that at least a single UV filter – probably akin to UVF3 – was present in the common ancestor of all included species. Based on the reconstruction of the number of filters in each species (Fig. 3A) there have since been at least three independent events of gains of additional filter types, and three of loss of complexity in the UV filter set. UV filters have apparently been lost altogether in lysiosquilloids, but are present in the three other included superfamilies. The UVF2 and UVF4 filters are only found in gonodactyloids, suggesting an elaboration of the ancestral filter set in this superfamily (Fig. 3B).

Correlation of spectral properties of UVF2 and UVF3 with habitat depth

We examined the relationship between the habitat depth of stomatopod species and spectral properties of their filters. By plotting the λ_{\max} of each filter versus that species' maximum

habitat depth (Fig. 4A), we found the λ_{\max} of UVF2 and UVF3 short-pass filters tended to shift towards longer wavelengths as the species' habitat depth increased. This logarithmic correlation was significant even when corrected for similarities in values due to species' phylogenetic relatedness using phylogenetic generalized least squares (PGLS) analysis (UVF2 adjusted $R^2=0.45$, $P=0.0281$; UVF3 adjusted $R^2=0.33$, $P=0.0059$). In order to determine whether filter absorption varied with habitat depth among individuals of a species, we examined the UV filters of *Haptosquilla trispinosa* captured either from the intertidal zone or from a depth of 20 m. We found that the absorbance spectrum and OD of UVF3 (the only primary UV filter expressed in this species) in the two populations was nearly identical (Fig. 4B). We also carried out an experiment where *H. trispinosa* individuals were captured from intertidal reef flats and either kept in natural light or complete darkness for 14 days without food. We found that the filters possessed the

Table 1. Summary of UV crystalline cone filter pigments in stomatopods

Species	Primary filters					F no.	Secondary filters			
	UVF1 Row 1,2	UVF2 Row 3	UVF3 Row 4	UVF4 Row 5,6	Row 5,6		Row 2,3	DP	VP	
GONODACTYLOIDEA (G)										
Gonodactylidae (g)										
<i>Gonodactylaceus falcatus</i> (Gf)	332	375	376	308	4	384	–	–	–	
Forskål 1775	5,2,1.13	3,2,1.32	4,3,1.62	3,1,2.32		3,2,0.40				
<i>Gonodactylaceus tematensis</i> (Gt)	331	376	376	301	4	+	–	–	–	
de Man 1902	3,1,0.63	1,1,0.71	4,1,0.45	3,1,0.71						
<i>Gonodactylellus affinis</i> (Ga)	334	372	371	301	4	376	–	–	–	
de Man 1902	4,3,0.76	1,1,1.65	1,1,1.01	1,1,0.98		1,1,0.50				
<i>Gonodactylellus viridis</i> (Gv)	340	362	371	308	4	389	–	–	–	
Serène 1954	2,1,0.35	3,1,1.23	6,1,1.07	4,1,1.34		4,1,0.15				
<i>Gonodactylus chiragra</i> (Gc)	–	370	373	306	3	386	–	357	–	
Fabricius 1781		3,2,1.19	4,3,2.12	4,2,1.00		4,2,0.37		2,1,0.23		
<i>Gonodactylus platysoma</i> (Gp)	334	358	361	309	4	+	–	–	–	
Wood-Mason 1895	8,5,0.78	13,5,2.87	6,5,1.61	7,3,2.17						
<i>Gonodactylus smithii</i> (Gs)	330	374	377	308	4	379	–	378	–	
Pocock 1893	9,5,0.95	4,4,1.40	6,4,1.63	4,2,1.67		4,2,0.24		1,1,0.21		
<i>Neogonodactylus oerstedii</i> (No)	332	372	375	308	4	388	–	360	–	
Hansen 1895	7,5,1.26	12,12,1.89	15,15,1.91	27,16,2.29		27,16,0.42		1,1,0.25		
<i>Neogonodactylus wenerae</i> (Nw)	–	370	378	304	3	384	–	+	–	
Manning & Heard 1997		2,1,1.95	3,1,0.84	4,1,2.00		4,1,0.08				
Odontodactylidae (o)										
<i>Odontodactylus havanensis</i> (Oh)	–	–	378	–	1	–	–	–	331	
Bigelow 1893			6,3,1.83						4,2,2.08	
<i>Odontodactylus latirostris</i> (OI)	–	–	380	–	1	–	–	–	–	
Borradaile 1907			3,1,1.31							
<i>Odontodactylus scyllarus</i> (Os)	336	301	385	302	4	–	–	–	–	
Linnaeus 1758	5,1,0.63	4,1,1.19	2,1,0.85	6,1,1.47						
Protosquillidae (pr)										
<i>Chorisquilla hystrix</i> (Ch)	–	–	381	–	1	–	385	–	–	
Nobili 1899			4,2,1.08				2,1,0.28			
<i>Chorisquilla tweediei</i> (Ct)	–	–	376	–	1	–	378	–	–	
Serène 1952			2,1,0.92				4,1,0.15			
<i>Haptosquilla glyptocercus</i> (Hg)	–	–	380	–	1	–	391	–	–	
Wood-Mason 1875			1,1,0.89				2,1,0.14			
<i>Haptosquilla trispinosa</i> (Ht)	–	–	380	–	1	–	378	–	–	
Dana 1852			9,5,0.98				7,5,0.25			
HEMISQUILLOIDEA (H)										
Hemisquillidae (h)										
<i>Hemisquilla californiensis</i> (Hc)	–	–	387	–	1	–	–	–	–	
Stephenson 1967			1,1,0.44							
LYSIOSQUILLOIDEA (L)										
Lysiosquillidae (l)										
<i>Lysiosquillina maculata</i> (Lm)	–	–	–	–	0	–	–	–	–	
Fabricius 1793										
Nannosquillidae (n)										
<i>Coronis scolopendra</i> (Cs)	–	–	–	–	0	–	–	–	–	
Latreille 1828										
PSEUDOSQUILLOIDEA (P)										
Pseudosquillidae (ps)										
<i>Pseudosquilla ciliata</i> (Pc)	333*	–	379	–	2	–	379	–	–	
Fabricius 1787	4,2,1.18		7,2,1.43				10,2,0.10			
<i>Pseudosquilliana richeri</i> (Pr)	–	–	379	–	1	–	–	–	–	
Moosa 1991			5,1,0.87							

Data are given as: the wavelength of filter maximum absorbance (λ_{\max} in nm, shown in bold) for primary and secondary UV filters, as defined in the text; below the λ_{\max} is n , i , OD_{\max} ; where n =the number of scans averaged, i =the number of individuals surveyed and OD_{\max} =the maximum optical density of the crystalline cone pigment through an end-on, 200 μ m section (see explanation in Materials and methods). Dashes indicate the absence of a discernible filter pigment. The total number of primary filters for each species (F no.) is also shown. Plus signs indicate that indicative autofluorescence was observed, but an absorbance spectra was not obtained.

*In Pc, UVF1 is found only in midband row 1.

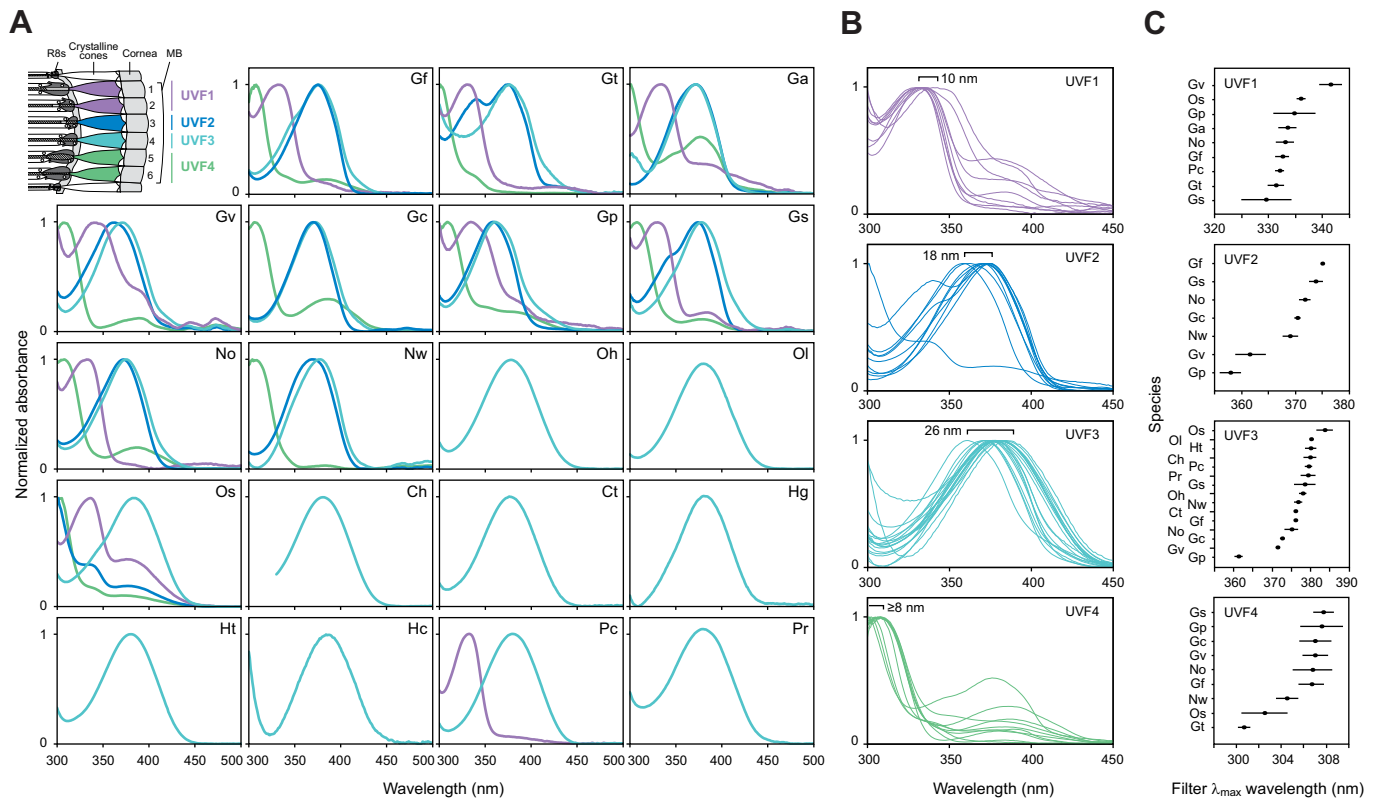


Fig. 2. Primary crystalline cone UV filter absorbance spectra in stomatopods. (A) The top-left panel diagrams the midband (MB, rows numbered) of a typical gonodactyloid stomatopod. The diagram is oriented as the section in Fig. 1C. In each ommatidium, light enters through the cornea, passes through the crystalline cones and enters the eighth reticular cells (R8s), which are sensitive to UV light. The crystalline cones are colored to indicate the four primary UV filter types (UVF1–4). Filters UVF2–4 are colored to match their fluorescent emission (see Fig. 1C), while the UVF1 did not fluoresce under our illumination conditions and is colored purple arbitrarily. Spectral plots show normalized averaged absorbance spectra of the crystalline cones in 19 species of stomatopods. Refer to Table 1 for species abbreviations and absorption data values. Species that were found to not have UV-absorbing pigments in their crystalline cones are not shown. The traces are colored according to primary filter type as in the top-left diagram. (B) Normalized averaged absorbance spectra from the four primary UV filters in each species of stomatopod. Spectral plots are colored according to A and the brackets indicate the wavelength of maximum absorption (λ_{\max}) range among species. (C) Mean (\pm s.e.) λ_{\max} values for each species of stomatopod (refer to Table 1 for species abbreviations). Species with only a single filter scan are omitted.

original OD in both groups, and were spectrally identical (Fig. 4C).

Other UV filter types

Our survey uncovered additional filter types in crystalline cones beyond the four primary filters already discussed in the midband (Fig. 5). In the protosquillids (*H. trispinosa*, *Haptosquilla glyptocercus*, *Chorisquilla tweediei* and *Chorisquilla hystrix*) and the distantly related pseudosquilloid *Pseudosquilla ciliata*, midband rows 2 and 3 dimly fluoresce cyan–green, similar in emission color to UVF3 (Fig. 5A and Fig. 11, J). There is a weakly absorbing pigment in these rows with a λ_{\max} between 378 and 391 nm (Fig. 5A, Table 1). In a more dramatic case, in the first 10 rows of the ventral periphery adjacent to the midband, *Odontodactylus havanensis* expresses a very dense filter akin to UVF1 (Fig. 5B, Table 1). Finally, several gonodactylids (*N. oerstedii*, *Neogonodactylus wenerae*, *Gonodactylus smithii* and *Gonodactylus chiragra*) were found to have blue-emitting fluorophores in the first few rows of crystalline cones in the dorsal periphery adjacent to the midband (Fig. 5C, large arrowhead). The pigments in these cones were difficult to measure, but they had a λ_{\max} near 360 nm (Fig. 5C). In *G. smithii*, this blue-fluorescing pigment was found not only in the crystalline cones of the dorsal periphery adjacent to the midband but also in the crystalline cones in the dorsal-most region of the eye (Fig. 5C, small arrowhead).

Development

In order to look at the developmental origin of these pigments, we examined an individual *Haptosquilla* postlarva, which is one of the developmental stages where the adult retina is actively being built alongside the degenerating larval retina (Cronin et al., 1995; Feller et al., 2015; Jinks et al., 2002). Under 375 nm illumination, the postlarva exhibited UV-stimulated autofluorescence in the adult eye midband consistent with the row 4 UVF3 fluorophore typical of adult *Haptosquilla* (Fig. 6). The dim secondary filter fluorophore in rows 2 and 3 was also present. These fluorescent pigments appeared to generally aggregate over the degrading larval retina at the advancing edge of the developing adult retina, before being sequestered into specific crystalline cones of the adult midband.

DISCUSSION

Diversity of primary UV filters in stomatopods

As suggested by the variety of UV-excited fluorescent emission spectra observed in stomatopod eyes (Fig. 1), a great diversity of strong, optically effective UV filters exists in the crystalline cones of stomatopods (Fig. 2, Table 1). Based on these observations, we classified the UV filters into four ‘primary’ filter types. In certain species, we also observed ‘secondary’ UV filter pigments in the midband and periphery, which will be discussed in detail below. The four primary UV filters are referred to here as UVF1–4.



Fig. 3. Ancestral state reconstructions of primary UV filters in stomatopod eyes. The phylogeny and reconstruction techniques are based on the analysis and methods published in Porter et al. (2010), with the addition of new species included in this study. Refer to Table 1 for taxonomic abbreviations. (A) Ancestral state reconstruction of the total number of primary UV filter types found in the crystalline cones of each species. Circled plus and minus symbols indicate potential events of loss or gain of UV filter types. (B) Ancestral state reconstruction of the presence or absence of each of the four primary UV filter types. Coloration refers to Fig. 2. Asterisks refer to atypical filter expression (see explanation in Discussion).

UVF1, found in midband rows 1 and 2, usually has an absorption spectrum similar to porphyra-334, with a λ_{\max} near 334 nm, and does not fluoresce at human-visible wavelengths. UVF1 was found in *P. ciliata* (where it atypically appears only in row 1), *Odontodactylus scyllarus* and most gonodactylids excepting *G. chiragra* and *N. wennerae*. UVF1 is often relatively weakly absorbing compared with the other primary filters, with maximum densities through 200 μm crystalline cone sections typically under OD 1.0, ranging from 0.35 to 1.53. In stomatopods this filter likely acts as a long-pass filter in both midband rows (see Materials and methods for an explanation of assumptions regarding UV visual pigment absorbances in stomatopods).

UVF2 occurs in midband row 3 and has λ_{\max} values between 358 and 376 nm. UVF2 fluoresces blue when stimulated with 375 nm UV light (Fig. 1A–F). In most species, this filter is likely produced by an uncharacterized MAA similar to pigments that have been observed in the lens of teleost fish (Thorpe et al., 1993). In *Gonodactylus platysoma* and *Gonodactylellus viridis*, however, UVF2's absorbance spectrum is very similar to that of the MAA palythene ($\lambda_{\max}=360$ nm). UVF2 is found exclusively in gonodactylids, and primarily in the family Gonodactylidae, where all species examined by MSP had this pigment. However, *Gonodactylellus annularis*, which was only observed by fluorescent emission, lacks a fluorophore in any midband row suggesting that UVF2 is absent in that species (supplementary

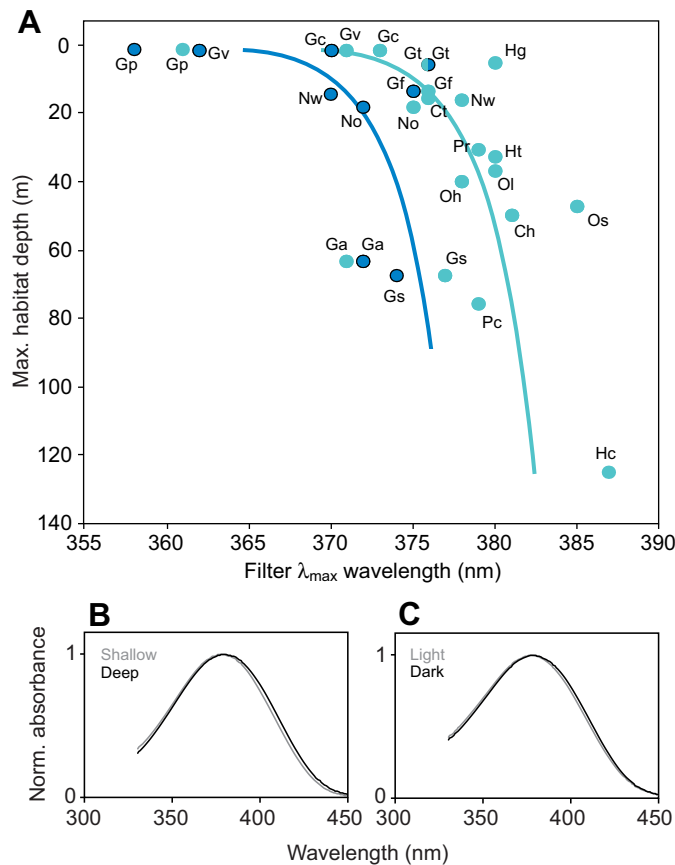


Fig. 4. The relationship of UV filter absorbance with stomatopod species habitat depth. (A) The λ_{\max} of UVF2 (blue markers) and UVF3 (cyan markers) short-pass filter pigments versus maximum habitat depth for each species. Logarithmic best-fit lines (colored to match the markers) suggest a relationship between filter λ_{\max} and increasing habitat depth. This correlation is confirmed by phylogenetic generalized least squares (PGLS) analysis, which corrects for similarities in values due to species relatedness (UVF2 $P=0.028$; UVF3 $P=0.006$; see explanation in Results and Materials and methods). Maximum habitat depth is computed from the average of maximum depths reported in Ah Yong (2001), Manning (1969) and Schram and Müller (2004), and from personal communications with Roy L. Caldwell. Species are indicated using two letter abbreviations as in Table 1. (B) The normalized absorbance spectra of UVF3 in *H. trispinosa* collected from shallow intertidal reefs (gray line, $\lambda_{\max}=378 \pm 0.50$ nm, mean \pm s.d., $N=4$) versus 20 m deep habitats (black line, $\lambda_{\max}=380 \pm 0.76$ nm, $N=7$). (C) The normalized absorbance spectra of UVF3 in shallow-caught *H. trispinosa* kept for 14 days in normal daylight (gray line, $\lambda_{\max}=378 \pm 1.19$ nm, $N=8$) versus darkness (black line, $\lambda_{\max}=378 \pm 1.32$ nm, $N=9$).

material Table S2). In most species, UVF2 occurs at maximum densities exceeding 1.0 with values as high as OD 2.89 (through 200 μ m crystalline cone sections), making for prodigious short-pass filtering effects. *Odontodactylus scyllarus* lacks a typical UVF2, and instead has a deep-UV-absorbing filter in row 3, more akin to UVF4.

UVF3 is found in midband row 4 and has a λ_{\max} between 361 and 387 nm. UVF3 fluoresces cyan or light green when illuminated with 375 nm UV light (Fig. 1A–J). Like UVF2, this filter is probably based on an uncharacterized MAA pigment. UVF3 is the most pervasive filter type in stomatopods, and is present in every species that has any UV filters in the crystalline cones (Fig. 2A). Like UVF2, it also appears to function as a strong short-pass filter, and has ODs as high as 2.80 in some species. Interestingly, though the UVF2 and UVF3 absorbance spectra often overlap among different species, the emission spectra of the two filters remain separate

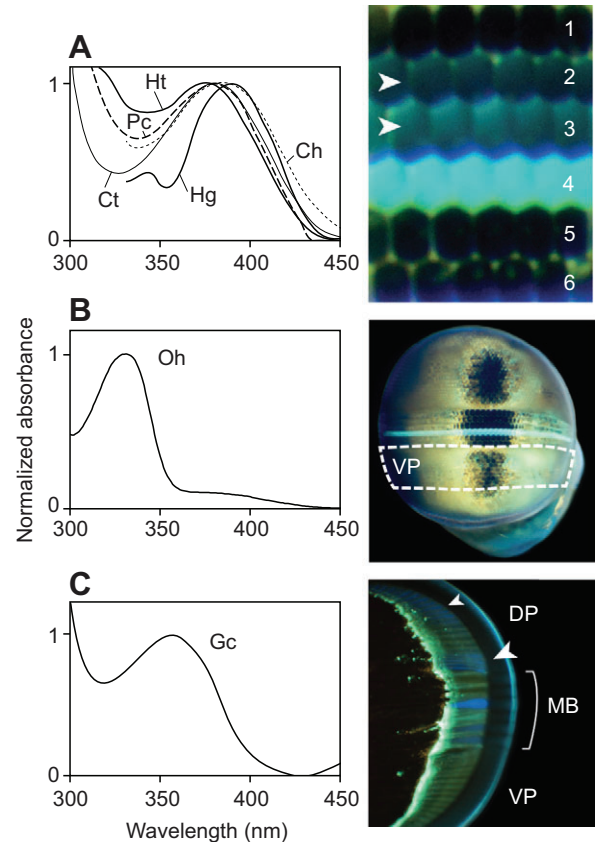


Fig. 5. Secondary UV filter pigments in the crystalline cones of stomatopods. (A) Normalized absorbance spectra (left panel; line thickness and dashes are intended to better differentiate the spectra; species abbreviations as in Table 1) of dim green fluorescent pigments found in midband (MB) rows 2 and 3 of *H. trispinosa* (right panel, rows 2 and 3 indicated with arrowheads), *Haptosquilla glyptocercus*, *C. hystrix*, *Chorisquilla tweediei* and *Pseudosquilla ciliata*. (B) Normalized absorbance spectra of UV filter pigment found in the ventral periphery (VP) of *Odontodactylus havanensis* (right panel with white outlined region indicating the ommatidia containing this non-fluorescing pigment). Note that the pigmented region covers the VP pseudopupil when the eye is oriented directly at the observer. (C) Normalized absorbance spectra of the blue fluorophore (right panel, large arrowhead) found in the dorsal periphery (DP) crystalline cones of some gonodactylids. The absorbance spectrum shown is from *G. chiragra*, but the fluorophore has also been observed in *Gonodactylus smithii* (right panel), *N. oerstedii* and *N. wenneerae*. Note that in *G. smithii*, the fluorophore is also present in the dorsal-most crystalline cones of the DP (right panel, small arrowhead).

(supplementary material Fig. S1), suggesting that two distinct pigment types produce these filters.

UVF4 exists in rows 5 and 6 of the midband and has a λ_{\max} between 301 and 309 nm. In most species, UVF4F seems to be primarily composed of mycosporine-glycine ($\lambda_{\max}=310$ nm), but *Gonodactylus affinis*, *Gonodactylaceus ternatensis*, *Gonodactylaceus falcatus* and *O. scyllarus* all have shorter-wavelength-absorbing UVF4 pigments. The primary UVF4 pigment does not fluoresce at visible wavelengths under 375 nm illumination, but midband rows five and six typically have a fluorescent secondary pigment absorbing much more weakly at λ_{\max} values between 376 and 389 nm and fluorescing light blue or green (Fig. 1A–E,K). In our survey, the green fluorescence from the secondary pigment was diagnostic for the presence of the primary UVF4 filter in these rows. However, in *N. wenneerae* (Fig. 1C) and *O. scyllarus*, the primary UVF4 pigment is present even when the

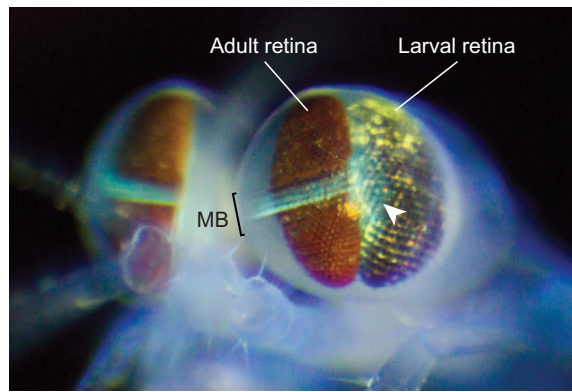


Fig. 6. UV filters in postlarval *Haptosquilla* sp. This juvenile of indeterminate sex was light trapped in the water column at night, indicating that it had not yet settled to a benthic adult lifestyle. The adult retina is still developing (advancing left to right in the image), taking the place of the degenerating larval retina. Upon stimulation with 375 nm UV light, green fluorescent emission in midband (MB) rows 2–4 indicates the presence of the typical row 4 UVF3 filter pigment as well as the row 2 and 3 secondary pigment found in adult protosquillids. The green fluorescent pigment that is sequestered into the MB crystalline cones of the adult retina appears to aggregate over the larval retina at the advancing edge of the developing adult retina (white arrowhead).

secondary fluorophore is not (Fig. 2A). We encountered UVF4 only in the Gonodactyloidea, specifically in all gonodactylids and also *O. scyllarus*. UVF4 acts as a long-pass filter in conjunction with the secondary short-pass filter (when present), creating a notch filter.

The widespread occurrence of these four UV filter types suggests a degree of consistency in the UV tuning system of stomatopods. Of the 21 species examined by MSP, only two (*Lysiosquillina maculata* and *Coronis scolopendra*) had no detectable UV-absorbing pigments in the crystalline cones. The remaining 19 species all had at least UVF3 in midband row 4. Also, with the exception of the unusual UVF2 pigment in *O. scyllarus* row 3, all primary filters are essentially similar pigments with similar probable filtering functionality. This suggests that the filters first appeared during the early radiation of stomatopod superfamilies, and raises questions about the evolution of the diversity of filters observed in extant species.

Evolution of UV filters in stomatopods

Our character state reconstruction suggests that the ancestral stomatopod eye likely had at least one UV filter (Fig. 3A). Ancestral state reconstructions of the individual primary filters indicate that this ancestral UV filter was most likely to be UVF3, located in midband row 4 (Fig. 3B). UVF3 is also found in *Hemisquilla californiensis*, which is thought to represent a basal lineage amongst modern stomatopods (Ahyong and Jarman, 2009; Porter et al., 2010). The four UV filter classes found in the gonodactylids are apparently an elaboration unique to that family. The unusual nature of the UV filters in *O. scyllarus* implies that this species may have come to its elaborate UV filter set independently of the diversification in the gonodactylids. Our reconstruction also suggests that the absence of UV filters in lysiosquilloids represents a loss of ocular complexity in that superfamily, as it is nested among the hemisquilloids, pseudosquilloids and the gonodactylids, all of which have UV filters. This loss of optical filtering complexity in the lysiosquilloids is consistent with the results of Porter et al.'s (2010) study of the intrarhabdomal long-wavelength filters, which also found a reduction of filter types in this group. The only other loss of UV filter diversity indicated by our reconstruction involves

the loss of UVF1 in *G. chiragra* and *N. wennerae* from a gonodactylid ancestor that likely possessed all four UV filters.

Also of note is the UVF1 filter in *P. ciliata*. If only UVF3 were present in the common ancestor of the pseudosquilloids and gonodactylids, it is surprising that both lineages independently stumbled upon a porphyra-334-like MAA for use in a UVF1 filter. However, *P. ciliata* is the only species we encountered in which UVF1 is expressed only in midband row 1. Perhaps, as porphyra-334 is potentially a precursor to most of the UV filters in stomatopods (Bok et al., 2014), it has been incorporated independently on multiple occasions. Additional taxon sampling in the pseudosquilloids, odontodactylids and protosquillids could better resolve these unusual cases.

Spectral diversity and ecology of UV filters in stomatopods

As we have shown here, the four primary filter classes are quite rigid in their location within the midband, general filtering effect and spectral shape within single species (Fig. 2). Between species, however, the spectral properties of the filter classes do exhibit considerable variability (Fig. 2B). UVF1 is fairly consistent among species, appearing to conform mostly to the absorbance of porphyra-334 ($\lambda_{\max}=334$ nm). However, in *G. platysoma* and *G. viridis* this filter has a broader red-shifted spectrum, perhaps owing to the inclusion of additional pigments (or elevated prominence of scattering effects caused by low pigment density in the case of *G. viridis*). UVF2 has a consistently shaped absorbance spectrum that nevertheless varies in λ_{\max} from 358 nm in *G. platysoma* to 376 nm in *G. ternatensis* (excepting the strange midband row 3 pigment in *O. scyllarus*). Similarly, UVF3 also varies among species, from $\lambda_{\max}=361$ nm in *G. platysoma* to 387 nm in *H. californiensis*. Finally, in most species with UVF4, the filter seems to be based on mycosporine-glycine ($\lambda_{\max}=310$). However, *Gonodactylaceus falcatus*, *G. ternatensis*, *O. scyllarus* and *G. affinis* all have UVF4s with shorter-wavelength absorbance spectra. Aside from shared evolutionary history, what factors could be the driving force behind this variability as well as the differences in primary filter number mentioned earlier?

To answer this question, we examined the absorbance spectra from UVF3 in various species. We noticed several trends that seemed to be related to the habitat depth range of the stomatopod species. The shorter-wavelength-absorbing variants of this filter seemed to be found primarily in species that lived exclusively in shallow habitats (*G. platysoma*, *G. chiragra* and *G. viridis*), while species living in deeper habitats (*H. californiensis*, *O. scyllarus* and *C. hystrix*) tended to have the reddest-shifted UVF3 pigment variants. Additionally, the deeper-living *H. californiensis* had the lowest recorded UVF3 optical density. Finally, we noticed that species that lived at greater depths tended to have fewer filter types. Taken together, these observations imply that species' habitat depth range influences the tuning, density, and number of their UV filters. We hypothesize that as short-wavelength UV light is attenuated rapidly in the aquatic environment at increasing depths (Jerlov, 1976), stomatopod UV optical pigments are tuned or lost in order to filter deep UV light less aggressively, thus maintaining a polychromatic UV visual system, without driving photoreceptor sensitivity below the threshold for function in the available environmental UV light.

In order to learn whether UV filter tuning correlates with species habitat depth, we plotted the λ_{\max} of UVF2 and UVF3, the two primary short-pass filters, from each species versus that species' mean habitat depth (Fig. 4A) (Ahyong, 2001; Manning, 1969; Schram and Müller, 2004). The results are consistent with our hypothesis that habitat depth plays a role in the evolutionary spectral

tuning of UV filters; longer λ_{\max} filters are found more regularly in deeper-dwelling species, independent of phylogenetic relationships. Interestingly, this distribution is best fitted with logarithmic trend lines, echoing the logarithmic attenuation of light in water. UVF2 is also less commonly present as mean habitat depth increases. The primary outliers in this analysis are *G. smithii* and *G. affinis*, both of which exhibit shorter λ_{\max} filters than other species with their mean depth. Both of these species are found over a great range of depths, from intertidal and littoral reefs to depths of over 60 m, but all the individuals from these species included in this analysis were caught at depths of less than 2 m. Finally, it is interesting that UVF3 is preserved in primarily deep-dwelling species, albeit in a red-shifted state. This suggests an important ecological function for spectrally tuning UV receptors to short wavelengths in the UV.

We also tested whether species that live at a great range of depths spectrally tuned their UV filters in response to their residential depth, or whether instead the spectral characteristics of the filters are fixed within a species. We collected *H. trispinosa* from 20 m and from shallow intertidal reef flats at Lizard Island in Australia. We found that the absorbance spectra of UV3F in these two *H. trispinosa* populations were essentially identical (Fig. 4B), but the λ_{\max} (mean \pm s.e.) of the two populations varied between 378 ± 0.50 nm in shallow-caught individuals and 380 ± 0.76 nm in deep-caught individuals. This degree of tuning is functionally irrelevant and is not consistent with the much broader spectral tuning in this filter seen among different species. We also carried out an experiment in which *H. trispinosa* were collected in intertidal habitats and placed in laboratory aquaria. Half of the animals were left in normal daylight, while the other half were placed in complete darkness for 2 weeks. The animals were not fed during this time. After 14 days, their UVF3 filters were measured (Fig. 4C). For both populations the absorption spectra remained identical to those of freshly shallow-caught animals, at $\lambda_{\max}=378$ nm. This result suggests that if the filter is tuned in low light environments, any changes require longer than 2 weeks, and that the pigment that contributes to UVF3 is fairly photostable and persistent, as its density did not decrease noticeably after 2 weeks in either population without dietary input.

Secondary UV filters

In addition to the four primary UV filter types discussed previously, we also identified several ‘secondary’ UV filters in the crystalline cones of various species (Fig. 5). Here, we discuss the spectral properties of these filters and examine their potential uses, evolutionary trends and ecological significance.

In all four protosquillid species examined here, as well as *P. ciliata*, we noticed a dim green fluorophore in the crystalline cones of midband rows 2 and 3 (Fig. 1F,G, Fig. 5A). There are no primary filters in these rows; protosquillids only have UVF3 in row 4, and *P. ciliata* has UVF3 in row 4 and UVF1 in row 1 only. The absorbance spectrum of this weak pigment was measured in all five of these species (Fig. 5A), and it was found to have a λ_{\max} between 378 and 391 nm, putting it in similar general wavelength range as the UVF3 pigment in these species. It could be that this pigment in rows 2 and 3 is the same as UVF3. It is not a strong absorber, with a maximum density not exceeding OD 0.28, so it likely does not have a strong effect on R8 spectral tuning in these rows. However, this pigment is interesting in that it occurs in very distantly related species, including protosquillids and the pseudosquillid *P. ciliata*, suggesting some well-conserved function.

UV filters were also found in the crystalline cones of the peripheral retinas of some species. In *O. havanensis*, the first 9 or 10

rows of the ventral periphery (adjacent to the midband) contain a strong pigment that is spectrally related to porphyra-334 UVF1 pigments (Fig. 5B). This pigment has a λ_{\max} at 331 nm and an OD_{max} of 2.08. Interestingly, the peripheral crystalline cones that express this pigment nicely cover the pseudopupil in that region when the eye is oriented directly at the observer (Fig. 5B). Therefore, as the ommatidia from both peripheral regions and the midband image the same area of space in this orientation, this pigment could create a UV color vision system between the peripheral regions without input from the midband.

UV filters are also found in the dorsal periphery of certain gonodactylids. When examining crystalline cone fluorescence patterns in eye cross-sections, we noticed that in some species, crystalline cones in the first few rows of the dorsal periphery adjacent to the midband exhibited blue fluorescence when stimulated with 375 nm UV light, akin to the UVF2 pigment in midband row 3 (Fig. 5C, large arrowhead). This has been observed in *N. oerstedii*, *N. wennerae*, *G. smithii* and *G. chiragra*. It proved to be very difficult to record absorbance spectra from these crystalline cones as they are so narrow and distort heavily when sectioned, but we were able to record a few scans from *G. chiragra* and *N. oerstedii* (Fig. 5C). The λ_{\max} of this pigment was near 360 nm, with a weak OD_{max} of 0.25. Interestingly, the crystalline cones expressing this pigment actually point at a slight downward angle, across the midband’s field of view (Marshall and Land, 1993), so they do not image the same point in space as the midband and ventral periphery (as was the case for the ommatidia containing pigment in the ventral periphery of *O. havanensis*). This could imply a different function for this pigment, perhaps acting as an ‘eye-shade’ to keep off-axis UV light from entering the midband crystalline cones from above, as is seen in the UV-screening dorsal corneal pigments of some teleosts (Douglas, 1989; Muntz, 1982). This is reasonable as the heavily tuned R8 UV receptors of the midband are likely very insensitive to UV light, so it would benefit the eye to minimize scattered UV light from laterally entering the midband R8 rhabdoms. Furthermore, in *G. smithii* only, there are additional crystalline cones with this blue fluorescent pigment in the dorsal region of the dorsal periphery (Fig. 5C, small arrowhead). It could be that these pigments are being used as photo-protectants against down-welling UV light. It is even possible that the primary UV filters in the midband originated as ocular photoprotectants – the role most commonly associated with MAAs in nature – and they were subsequently exploited for UV spectral tuning in stomatopods.

The discovery of UV filter pigments in the peripheral hemispheres of stomatopod eyes supports the notion that these regions are not completely homogeneous arrays of ommatidia used solely for spatial vision. Together with the finding that the R8s in the dorsal and ventral peripheries express two different opsin transcripts (Bok et al., 2014), these specializations suggest additional roles for the peripheral hemisphere ommatidia, including contributing to UV color vision. It is interesting that the peripheral UV-absorbing filter pigments are found directly adjacent to the midband. It is as if the extreme retinal specialization typical to the midband is ‘leaking’ into the adjacent ommatidia. However, this observation could be a by-product of an incomplete survey of the peripheral crystalline cones that were not directly adjacent to the primary area of investigation. It is possible that many additional, non-fluorescent UV-absorbing pigments in the periphery simply evaded our notice.

Development of UV filters

We found that stomatopods possess UV optical filters at an early stage in their post-larval development. In stomatopods, the adult eye

actually develops *de novo* alongside the degenerating larval eye during late larval developmental stages (Cronin et al., 1995; Feller et al., 2015; Jinks et al., 2002), and the newly developing retina already includes the long-wavelength filter classes found in the main rhabdoms. Unsettled pelagic *Haptosquilla* postlarvae were observed to already have UVF3 as indicated by fluorescent emission in row 4 of the midband, as well as the row 2 and 3 secondary filters (Fig. 6). This suggests that MAA filters are incorporated into the crystalline cones early in development, perhaps as soon as the adult eye develops during late larval stages. Additional observations are required from larval developmental stages, as well as longer-term experiments where postlarvae are reared in variable ambient UV light environments similar to previous studies on the long-wavelength colored filters in the main rhabdoms (Cheroske et al., 2003; Cronin et al., 2001).

Summary and conclusions

Stomatopods are recognized as having complex and variable visual systems, well suited for an active social and predatory lifestyle. Here, we have shown that this complexity extends to the unique UV filters recently identified in the crystalline cones. Stomatopods express a variety of UV-absorbing pigments in various complements to form these UV filters. Furthermore, the UV filters were probably present in early stomatopods, and they have since been elaborated, and occasionally lost, over evolutionary history. The UV filters also seem to be tuned such that shallow-water species have more aggressively tuned UV photoreceptors in an environment with abundant UV light, while deep-living species have fewer, red-shifted filter pigments that maintain receptor sensitivity when less UV light is available. Finally, in some species, UV filter complexity extends beyond the midband, into the peripheral hemispheres, implicating these regions in more complex UV visual tasks than previously thought. These results further emphasize the importance of a highly tuned UV visual system for stomatopods. However, we still do not know how, and for what ecological tasks, stomatopods actually use this visual capacity. Future behavioral and ecological investigations will aim to better understand the role of UV vision in stomatopod predation, mate choice, species identification and aggression.

MATERIALS AND METHODS

Taxon sampling

Twenty-eight stomatopod taxa were examined in this analysis. This group represented the four superfamilies that have the most complex eye designs, with six specialized midband rows: Gonodactyloidea, Lysiosquilloidea, Pseudosquilloidea and Hemisquilloidea. The majority of the studied stomatopod species were captured at Lizard Island Research Station (QLD, Australia) by various collection techniques. Additional species were collected at Catalina Island (CA, USA), Moorea (French Polynesia) and the Florida Keys (USA), as well as purchased from tropical marine life distributors. Species were identified based on anatomical characteristics. The UV filters from animals collected at Lizard Island were either analyzed in the field using imaging spectroscopy or returned to the laboratory and analyzed using MSP. Both techniques are described in detail below, and there were no discernible differences in absorbance spectra for species that were examined using the two methods. All other animals were examined in the laboratory using MSP.

Fluorescence photography

Dissected whole eyes were affixed to a goniometer using superglue and the eyes were oriented to permit focusing directly on the midband with a dissecting microscope. The microscope was focused such that the depth of field extended from the surface of the eye, through the crystalline cones and into the distal tip of the rhabdoms, producing dark pseudopupils in the midband and both peripheral hemispheres. When possible, the eye was

rotated to visualize the enlarged pseudopupils in the acute zone of the eye. The eye was illuminated with two identical UV LEDs (no. LED370E, Thor Labs, NJ, USA) positioned on either side of the eye at roughly 45 deg relative to the surface of the eye. Exposures were taken with a Canon T2i DSLR using a microscope adaptor lens. Raw photos were globally manipulated for exposure, contrast and noise reduction, and backgrounds were subtracted. Eye cross-sections (200 μm) were prepared by vibratome sectioning as described in Bok et al. (2014) and fluorescence was imaged using a compound fluorescence microscope producing 365 nm epi-illumination. Photographs were captured and processed as above. Six species were examined only by fluorescence photography, and the presence of UV filters in rows 3 and 4 as well as the long-wavelength secondary component of rows 5 and 6 was inferred from the presence or absence of the typical fluorescent emission in each row (supplementary material Table S1).

MSP

To examine the absorption spectra of the crystalline cone UV pigments, 200 μm sections through the crystalline cone layer of the eye were prepared by vibratome sectioning, and the sections were mounted in between two coverslips in filtered seawater. MSP was carried out according to methods described previously (Cronin, 1985; Cronin et al., 1994c), with modifications to the system to maximize the spectral range of UV wavelengths directed through the crystalline cones for measurement as described in Bok et al. (2014). We were able to obtain smooth and consistent absorbance spectra between 300 and 550 nm using this setup. All absorbance data presented in this analysis were collected using this MSP, except for those from *L. maculata*, *C. hystrix* and the experimental *H. trispinosa* discussed in the section on habitat depth, which were recorded using a field MSP at Lizard Island. This instrument was based on the portable MSP described in Loew (1982). A xenon arc light source was used, and the monochromator replaced with a housing placing a UG5 filter and an IR blocker in the optical path. An aperture was created with a pinhole in aluminium foil prior to the filters. A quartz prism was used to direct the beam through a sample between quartz glycerol immersion lenses (a pair of Zeiss 32X Ultrafluors). Absorbance was measured using Spectra Suite software and a QE6500 spectrometer (Ocean Optics, FL, USA) with a 200 μm fiber placed in the imaging plane above the microscope. This MSP was only functional down to about 330 nm, so it was not useful in characterizing the primary filter in rows 5 and 6. Whenever possible, all UV filter data presented here were compared between the main MSP and the portable MSP with fresh-caught animals, and no discrepancies were observed. This indicates that transportation of the animals to the laboratory did not seriously impact the spectral properties of the filters.

Absorbance spectral data were corrected for scattering through the thick sections by fitting and subtracting the baseline from the slope between 450 and 550 nm, where no pigments were ever observed in the crystalline cones. From each individual the cleanest scans (without severe short-wavelength scattering or post mortem pigment degeneration) for each filter type were selected, compared and averaged with data for other individuals of the same species. The λ_{max} for each filter in each species is reported in Table 1, along with the number of scans that were averaged, the number of individuals they were pooled from, and the maximum OD of the filter pigment observed in an end-on scan through a crystalline cone in transverse section. This approximation of OD is an unavoidable shortfall of measuring the absorbance spectra of these filters, which begin to leach out of the crystalline cones and degenerate when the cones are ruptured during sectioning, and the actual densities of these filters in life are likely higher than reported here (see Bok, 2013 and Bok et al., 2014 for additional details). Therefore, our analysis primarily concerns the presence or absence and the spectral absorbance of the pigments.

In discussing the role of the UV filters in spectral tuning in various species of stomatopods we assume that the UV visual pigment expression pattern reported in Bok et al. (2014) for *N. oerstedii* is mostly conserved in other stomatopods with six midband rows. Analyses of main rhabdom photoreceptors have shown that their visual pigment absorbance spectra are fairly invariant in comparison to the colored filters in those ommatidia (Cronin and Caldwell, 2002; Cronin et al., 2002). Electrophysiological and MSP studies of the R8s have also suggested conservation in visual

pigment absorbance spectra among species (Bok, 2013; Cronin et al., 1994c; Kleinlogel, 2004; Kleinlogel and Marshall, 2009; Thoen et al., 2014).

Phylogenetics and ancestral state reconstruction

DNA extraction, PCR and sequencing procedures were performed as described in Porter et al. (2010). New sequences were generated for species where data were not already available (supplementary material Table S2) and added to the data from Porter et al. (2010) for a dataset consisting of 47 stomatopod species. Representatives of three additional Eumalacostracan lineages were used to root the phylogeny (supplementary material Table S2). Each gene dataset was aligned separately using MAFFT v7 (Kato and Standley, 2013; Kato and Toh, 2008; Kato et al., 2005, 2002), concatenated, and highly divergent and/or ambiguous regions of the entire alignment were removed using GBLOCKS 0.91 (Castresana, 2000). The resulting alignment was used to estimate phylogenetic relationships and node confidence as bootstrap values using RAxML v7 (Stamatakis, 2006; Stamatakis et al., 2008) as implemented in the CIPRES portal (Miller et al., 2010). The resulting phylogeny was drawn using FigTree v1.4.0 (<http://tree.bio.ed.ac.uk/software/figtree/>).

Ancestral character states for the number of distinct types of UV filter pigments found in each species and the presence/absence of each type of filter pigment were reconstructed in Mesquite v2.75 (Maddison and Maddison, 2011), using the RAxML tree with species lacking filter pigment data pruned from the tree. All characters were assigned as standard categorical characters. Ancestral states for each character were inferred using Maximum Likelihood models and reconstructions were mapped onto the phylogeny.

The relationship between the λ_{\max} of UVF2 and UVF3 and the maximum depth of each species was determined using a PGLS method, which accounts for the shared evolutionary history of genes in calculating the correlation between characters. PGLS regressions were run in the caper package v0.5.2 (Orme et al., 2013) of the software program R v3.1.1 (R Core Team, 2014) as implemented in RStudio v0.98.994 (2012). For PGLS analyses, the habitat depth was taken as the averaged maximum recorded depth for each species reported in Ah Yong (2001), Manning (1969) and Schram and Müller (2004), and from personal communications with Roy L. Caldwell, and normalized by a \log_{10} transformation.

The effect of light environment on the UVF3 filter in *H. trispinosa*

Fifteen *H. trispinosa* individuals were captured in water less than 1 m deep at Lizard Island Research Station. They were split into three groups that were matched for sex and size. Five of the animals were killed immediately and their UV filters were examined by imaging spectrometry. Of the 10 remaining animals, five were placed in aquaria exposed to normal daylight, and the other five were placed in constant darkness. Both groups were not fed for this period, and after 14 days all animals were killed and their UV filters were measured using the field MSP. The average absorbance spectra from the three groups were then compared with one another as well as with *H. trispinosa* freshly caught at a depth of 20 m.

Acknowledgements

We are grateful to Sheila Patek and Roy Caldwell for collecting and sharing some animals used in this study (Patek funding: National Science Foundation no. 0641716 and National Geographic Society Committee for Research and Exploration). We thank Ellis Loew who graciously lent us his portable MSP for field measurements. We thank those who assisted with animal collection at Lizard Island (Kate Feller, Roy Caldwell, Justin Marshall and Hanne Thoen) and at Catalina Island (Brian Dalton). We thank the directors and staff at Lizard Island Research Station for facilitating our research. Thank you to Erin Sternhagen and Lee Wessel for help with generating additional sequence data for phylogenetic analyses.

Competing interests

The authors declare no competing or financial interests.

Author contributions

M.J.B. collected the data, carried out all the experiments and wrote the manuscript. M.L.P. constructed the stomatopod phylogeny, performed the character reconstruction and assisted with revising the manuscript. T.W.C. supervised the project and assisted with preparation of the manuscript.

Funding

This research was supported by funding from the Air Force Office of Scientific Research (FA9550-12-1-0321) and by the Lizard Island Research Station Isobel Bennett Marine Biology Fellowship awarded to M.L.P.

Supplementary material

Supplementary material available online at <http://jeb.biologists.org/lookup/suppl/doi:10.1242/jeb.122036/-/DC1>

References

- Ahyong, S. T. (2001). Revision of the Australian stomatopod crustacea. *Rec. Austr. Mus.* **26**, 1–326.
- Ahyong, S. T. and Jarman, S. N. (2009). Stomatopod interrelationships: preliminary results based on analysis of three molecular loci. *Arthropod Syst. Phylogeny* **67**, 91–98.
- Arikawa, K. and Stavenga, D. (1997). Random array of colour filters in the eyes of butterflies. *J. Exp. Biol.* **200**, 2501–2506.
- Arikawa, K., Mizuno, S., Scholten, D. G. W., Kinoshita, M., Seki, T., Kitamoto, J. and Stavenga, D. G. (1999a). An ultraviolet absorbing pigment causes a narrow-band violet receptor and a single-peaked green receptor in the eye of the butterfly *Papilio*. *Vision Res.* **39**, 1–8.
- Arikawa, K., Scholten, D. G. W., Kinoshita, M. and Stavenga, D. G. (1999b). Tuning of photoreceptor spectral sensitivities by red and yellow pigments in the butterfly *Papilio xuthus*. *Zoolog. Sci.* **16**, 17–24.
- Bailes, H. J., Robinson, S. R., Trezise, A. E. O. and Collin, S. P. (2006). Morphology, characterization, and distribution of retinal photoreceptors in the Australian lungfish *Neoceratodus forsteri* (Krefft, 1870). *J. Comp. Neurol.* **494**, 381–397.
- Bok, M. J. (2013). The physiological, ecological, and evolutionary basis of polychromatic ultraviolet sensitivity in stomatopod crustaceans. PhD thesis, University of Maryland, Baltimore County, USA.
- Bok, M. J., Porter, M. L., Place, A. R. and Cronin, T. W. (2014). Biological sunscreens tune polychromatic ultraviolet vision in mantis shrimp. *Curr. Biol.* **24**, 1636–1642.
- Caldwell, R. L. and Dingle, H. (1975). Ecology and evolution of agonistic behavior in stomatopods. *Die Naturwissenschaften* **62**, 214–222.
- Carreto, J. I. and Carignan, M. O. (2011). Mycosporine-like amino acids: relevant secondary metabolites. Chemical and ecological aspects. *Mar. Drugs* **9**, 387–446.
- Castresana, J. (2000). Selection of conserved blocks from multiple alignments for their use in phylogenetic analysis. *Mol. Biol. Evol.* **17**, 540–552.
- Cheroske, A. G., Cronin, T. W. and Caldwell, R. L. (2003). Adaptive color vision in *Pullosquilla litoralis* (Stomatopoda, Lysiosquilloidea) associated with spectral and intensity changes in light environment. *J. Exp. Biol.* **206**, 373–379.
- Cheroske, A. G., Barber, P. H. and Cronin, T. W. (2006). Evolutionary variation in the expression of phenotypically plastic color vision in Caribbean mantis shrimps, genus *Neogonodactylus*. *Mar. Biol.* **150**, 213–220.
- Chiou, T.-H., Kleinlogel, S., Cronin, T., Caldwell, R., Loeffler, B., Siddiqi, A., Goldizen, A. and Marshall, J. (2008). Circular polarization vision in a stomatopod crustacean. *Curr. Biol.* **18**, 429–434.
- Cronin, T. W. (1985). The visual pigment of a stomatopod crustacean, *Squilla empusa*. *J. Comp. Physiol. A* **156**, 679–687.
- Cronin, T. W. and Caldwell, R. L. (2002). Tuning of photoreceptor function in three mantis shrimp species that inhabit a range of depths. II. Filter pigments. *J. Comp. Physiol. A Sens. Neural Behav. Physiol.* **188**, 187–197.
- Cronin, T. W. and Marshall, N. J. (1989a). A retina with at least ten spectral types of photoreceptors in a mantis shrimp. *Nature* **339**, 137–140.
- Cronin, T. W. and Marshall, N. J. (1989b). Multiple spectral classes of photoreceptors in the retinas of gonodactyloid stomatopod crustaceans. *J. Comp. Physiol. A* **166**, 261–275.
- Cronin, T. W., Marshall, N. J. and Caldwell, R. L. (1993). Photoreceptor spectral diversity in the retinas of squilloid and lysiosquilloid stomatopod crustaceans. *J. Comp. Physiol. A* **172**, 339–350.
- Cronin, T. W., Marshall, N. J. and Caldwell, R. L. (1994a). The intrarhabdomal filters in the retinas of mantis shrimps. *Vision Res.* **34**, 279–291.
- Cronin, T. W., Marshall, N. J., Caldwell, R. L. and Shashar, N. (1994b). Specialization of retinal function in the compound eyes of mantis shrimps. *Vision Res.* **34**, 2639–2656.
- Cronin, T. W., Marshall, N. J., Quinn, C. A. and King, C. A. (1994c). Ultraviolet photoreception in mantis shrimp. *Vision Res.* **34**, 1443–1452.
- Cronin, T. W., Marshall, N. J., Caldwell, R. L. and Pales, D. (1995). Compound eyes and ocular pigments of crustacean larvae (Stomatopoda and Decapoda, Brachyura). *Mar. Freshwater Behav. Physiol.* **26**, 219–231.
- Cronin, T. W., Marshall, N. J. and Caldwell, R. L. (2000). Spectral tuning and the visual ecology of mantis shrimps. *Philos. Trans. R. Soc. B Biol. Sci.* **355**, 1263–1267.
- Cronin, T. W., Caldwell, R. L. and Marshall, J. (2001). Sensory adaptation: Tunable colour vision in a mantis shrimp. *Nature* **411**, 547–548.

- Cronin, T. W., Caldwell, R. L. and Erdmann, M. V.** (2002). Tuning of photoreceptor function in three mantis shrimp species that inhabit a range of depths. I. Visual pigments. *J. Comp. Physiol. A Sens. Neural. Behav. Physiol.* **188**, 179-186.
- Cronin, T. W., Bok, M. J., Marshall, N. J. and Caldwell, R. L.** (2014). Filtering and polychromatic vision in mantis shrimps: themes in visible and ultraviolet vision. *Philos. Trans. R. Soc. B Biol. Sci.* **369**, 20130032.
- Dingle, H. and Caldwell, R. L.** (1969). The aggressive and territorial behaviour of the mantis shrimp *Gonodactylus bredini* Manning (Crustacea: Stomatopoda). *Behaviour* **33**, 115-136.
- Douglas, R. H.** (1989). The spectral transmission of the lens and cornea of the brown trout (*Salmo trutta*) and goldfish (*Carassius auratus*) – effect of age and implications for ultraviolet vision. *Vision Res.* **29**, 861-869.
- Douglas, R. H. and Marshall, N. J.** (1999). A review of vertebrate and invertebrate ocular filters. In *Adaptive Mechanisms in the Ecology of Vision* (ed. S. N. Archer, M. B. A. Djamgoz, E. R. Loew, J. C. Partridge and S. Vallergera), pp. 95-162. Dordrecht: Kluwer Academic Publishers.
- Feller, K. D., Cohen, J. H. and Cronin, T. W.** (2015). Seeing double: visual physiology of double-retina eye ontogeny in stomatopod crustaceans. *J. Comp. Physiol. A* **201**, 331-339.
- Goldsmith, T. H., Collins, J. S. and Licht, S.** (1984). The cone oil droplets of avian retinas. *Vision Res.* **24**, 1661-1671.
- Harling, C.** (2000). Reexamination of eye design in the classification of stomatopod crustaceans. *J. Crust. Biol.* **20**, 172-185.
- Horridge, G. A.** (1978). The separation of visual axes in apposition compound eyes. *Philos. Trans. R. Soc. B Biol. Sci.* **285**, 1-59.
- Hylander, S. and Jephson, T.** (2010). UV protective compounds transferred from a marine dinoflagellate to its copepod predator. *J. Exp. Mar. Biol. Ecol.* **389**, 38-44.
- Jerlov, N. G.** (1976). *Marine Optics*. Amsterdam: Elsevier.
- Jinks, R. N., Markley, T. L., Taylor, E. E., Perovich, G., Dittel, A. I., Epifanio, C. E. and Cronin, T. W.** (2002). Adaptive visual metamorphosis in a deep-sea hydrothermal vent crab. *Nature* **420**, 68-70.
- Katoh, K. and Standley, D. M.** (2013). MAFFT multiple sequence alignment software version 7: improvements in performance and usability. *Mol. Boil. Evol.* **30**, 772-780.
- Katoh, K. and Toh, H.** (2008). Recent developments in the MAFFT multiple sequence alignment program. *Brief. Bioinformatics* **9**, 286-298.
- Katoh, K., Misawa, K., Kuma, K.-I. and Miyata, T.** (2002). MAFFT: a novel method for rapid multiple sequence alignment based on fast Fourier transform. *Nucleic Acids Res.* **30**, 3059-3066.
- Katoh, K., Kuma, K.-I., Toh, H. and Miyata, T.** (2005). MAFFT version 5: improvement in accuracy of multiple sequence alignment. *Nucleic Acids Res.* **33**, 511-518.
- Kleinlogel, S.** (2004). Neural connections behind the complex retina of the stomatopod (mantis shrimp). PhD thesis, School of Biomedical Sciences, The University of Queensland, Australia.
- Kleinlogel, S. and Marshall, N. J.** (2006). Electrophysiological evidence for linear polarization sensitivity in the compound eyes of the stomatopod crustacean *Gonodactylus chiragra*. *J. Exp. Biol.* **209**, 4262-4272.
- Kleinlogel, S. and Marshall, N. J.** (2009). Ultraviolet polarisation sensitivity in the stomatopod crustacean *Odontodactylus scyllarus*. *J. Comp. Physiol. A* **195**, 1153-1162.
- Loew, E. R.** (1982). A field-portable microspectrophotometer. *Methods Enzymol.* **81**, 647-655.
- Maddison, W. P. and Maddison, D. R.** (2011). Mesquite: a modular system for evolutionary analysis. Version 2.75 <http://mesquiteproject.org>.
- Manning, R. B.** (1969). *Stomatopod Crustacea of the Western Atlantic*. Miami: University of Miami Press.
- Manning, R. B., Schiff, H. and Abbott, B. C.** (1984). Eye structure and the classification of stomatopod Crustacea. *Zool. Scripta.* **13**, 41-44.
- Marshall, N. J.** (1988). A unique colour and polarization vision system in mantis shrimps. *Nature* **333**, 557-560.
- Marshall, N. J. and Land, M. F.** (1993). Some optical features of the eyes of stomatopods. *J. Comp. Physiol. A* **173**, 583-594.
- Marshall, N. J. and Oberwinkler, J.** (1999). Ultraviolet vision: The colourful world of the mantis shrimp. *Nature* **401**, 873-874.
- Marshall, N. J., Land, M. F., King, C. A. and Cronin, T. W.** (1991a). The compound eyes of mantis shrimps (Crustacea, Hoplocarida, Stomatopoda). I. Compound eye structure: the detection of polarized light. *Philos. Trans. R. Soc. B Biol. Sci.* **334**, 33-56.
- Marshall, N. J., Land, M. F., King, C. A. and Cronin, T. W.** (1991b). The compound eyes of mantis shrimps (Crustacea, Hoplocarida, Stomatopoda). II. Colour pigments in the eyes of stomatopod crustaceans: polychromatic vision by serial and lateral filtering. *Philos. Trans. R. Soc. B Biol. Sci.* **334**, 57-84.
- Miller, M. A., Pfeiffer, W. and Schwartz, T.** (2010). Creating the CIPRES Science Gateway for inference of large phylogenetic trees. In *Gateway Computing Environments Workshop*, pp. 1-7. New Orleans, LA: IEEE.
- Muntz, W. R.** (1982). Visual adaptations to different light environments in Amazonian fishes. *Rev. Can. Biol. Exp.* **41**, 35-46.
- Newman, S., Dunlap, W., Nicol, S. and Ritz, D.** (2000). Antarctic krill (*Euphausia superba*) acquire a UV-absorbing mycosporine-like amino acid from dietary algae. *J. Exp. Mar. Biol. Ecol.* **255**, 93-110.
- Orme, D., Freckleton, R., Thomas, G., Petzoldt, T., Fritz, S., Isaac, N. and Pearce, W.** (2013). Caper: comparative analyses of phylogenetics and evolution in R. R package version 0.5.2. <http://CRAN.R-project.org/package=caper>.
- Porter, M. L., Bok, M. J., Robinson, P. R. and Cronin, T. W.** (2009). Molecular diversity of visual pigments in Stomatopoda (Crustacea). *Visual Neurosci.* **26**, 255-265.
- Porter, M. L., Zhang, Y., Desai, S., Caldwell, R. L. and Cronin, T. W.** (2010). Evolution of anatomical and physiological specialization in the compound eyes of stomatopod crustaceans. *J. Exp. Biol.* **213**, 3473-3486.
- Porter, M. L., Speiser, D. I., Zaharoff, A. K., Caldwell, R. L., Cronin, T. W. and Oakley, T. H.** (2013). The evolution of complexity in the visual systems of stomatopods: insights from transcriptomics. *Integr. Comp. Biol.* **53**, 39-49.
- R Core Team.** (2014). R: A language and environment for statistical computing. R Foundation for Statistical Computing, Vienna, Austria. URL <http://www.R-project.org/>.
- RStudio** (2012). RStudio: Integrated development environment for R (Version 0.96.122) [Computer software]. Boston, MA. Retrieved May 20, 2012. Available from <http://www.rstudio.org/>.
- Schiff, H., Abbott, B. C. and Manning, R. B.** (1986). Optics, range-finding, and neuroanatomy of the eye of a mantis shrimp, *Squilla mantis* Linnaeus. *Smithson. Contr. Zool.* **440**, 1-32.
- Schram, F. R. and Müller, H.-G.** (2004). *Catalog and Bibliography of the Fossil and Recent Stomatopoda*. Leiden: Backhuys.
- Shick, J. M. and Dunlap, W. C.** (2002). Mycosporine-like amino acids and related gadusols: biosynthesis, accumulation, and uv-protective functions in aquatic organisms. *Annu. Rev. Physiol.* **64**, 223-262.
- Stamatakis, A.** (2006). RAXML-VI-HPC: maximum likelihood-based phylogenetic analyses with thousands of taxa and mixed models. *Bioinformatics* **22**, 2688-2690.
- Stamatakis, A., Hoover, P. and Rougemont, J.** (2008). A rapid bootstrap algorithm for the RAXML Web servers. *Syst. Biol.* **57**, 758-771.
- Thoen, H. H., How, M. J., Chiou, T.-H. and Marshall, J.** (2014). A different form of color vision in mantis shrimp. *Science* **343**, 411-413.
- Thorpe, A., Douglas, R. H. and Truscott, R. J. W.** (1993). Spectral transmission and short-wave absorbing pigments in the fish lens—I. Phylogenetic distribution and identity. *Vision Res.* **33**, 289-300.
- Walls, G. L.** (1942). *The Vertebrate Eye and its Adaptive Radiation*. New York: Hafner Publishing Company.

SUPPLEMENTARY MATERIAL

Table S1. Summary of ultraviolet crystalline cone fluorophores, indicative of filter pigments, in stomatopods. Filters that are not typically fluorescent (e.g. UVF1 and UVF4) are omitted. Plus signs indicate that 375-nm-excited fluorescence was observed. Dashes indicate the absence of a fluorophore. Question marks indicate ambiguous observations. The estimated number of primary filters for each species (F#) is also shown.

Species	Primary filters		F#	Secondary filters		
	UVF2	UVF3		R5, 6	R2, 3	DP
GONODACTYLOIDEA						
Gonodactylidae						
<i>Gonodactylellus annularis</i> (Gn) Erdmann & Manning 1998	-	-	?	-	-	?
<i>Neogonodactylus austrinus</i> (Na) Manning 1969	+	+	≥ 2	?	-	?
<i>Neogonodactylus bredini</i> (Nb) Manning 1969	+	+	≥ 2	+	-	?
Odontodactylidae						
<i>Odontodactylus japonicus</i> (Oj) de Haan 1844	-	+	≥ 1	?	-	?
Takuidae						
<i>Taku spinosocarinatus</i> (Ts) Fukuda 1909	-	-	?	-	-	-
LYSIOSQUILLOIDEA						
Nannosquillidae						
<i>Alachosquilla vicina</i> (Av) Nobili 1904	-	-	?	-	-	-
<i>Pullosquilla thomassini</i> (Pt) Manning 1978	-	-	?	-	-	-

Table S2: Genbank accession numbers of new sequences (shown in bold) generated for phylogenetic analyses of stomatopod UV filter pigment evolution and of outgroup species used to root phylogenetic analyses. Stomatopod sequences with no accession numbers were available from Porter et al. 2010, and not shown here.

Taxon	COI	16S	18S	28S-1	28S-2
GONODACTYLOIDEA					
Gonodactylidae					
<i>Gonodactylus ternatensis</i>	KT001540	KT001543	KT001546	KY001548	KT001551
<i>Gonodactylellus viridis</i>	AF205224	KT001545	AY743947	KT001549	KT001552
<i>Neogonodactylus wennebaueri</i>	KT001541	KT001544	KT001547	KT001550	NA
Odontodactylidae					
<i>Odontodactylus havanensis</i>	KT001542	HM138840	HM138884	HM180028	HM180072
OUTGROUPS					
Syncarida					
<i>Anaspides tasmaniae</i>	DQ889076	AF133694	L81948	AY859549	NA
Mysida					
<i>Neomysis americana</i>	FJ581789	HM179997	HM179998	HM179999	NA
Eucarida					
<i>Euphausia eximia</i>	AY601080	DQ079713	DQ079748	DQ079787	NA

SUPPLEMENTARY FIGURE

A

Species	UVF2		UVF3	
	λ_{\max}	E_{\max}	λ_{\max}	E_{\max}
Ch	-	-	381	514
Ga	372	467	371	?
Gc	370	?	373	504
Gf	375	461	376	509
Gp	358	457	361	506
Gs	374	456	377	513
Hc	-	-	387	511
Ht	-	-	380	510
Hg	-	-	380	511
No	372	462	375	502
OI	-	-	380	508
Os	-	-	385	510
Pc	-	-	379	508
Average	370.17	460.60	377.31	508.83
s.d.	6.21	4.39	6.60	3.51

B

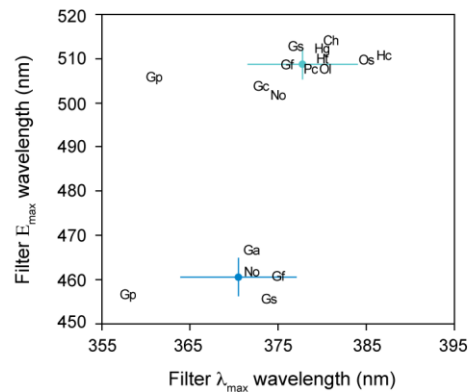


Fig. S1. Absorption and emission properties of filters UVF2 and UVF3. (A) A table displaying the wavelength of maximum absorbance (λ_{\max}) and emission (E_{\max} , measured as in Bok et al, 2014) for several stomatopod species (refer to Table 1 for abbreviations). Dashes indicate that the pigment is not present and question marks indicate that clear data was not obtained in this study. (B) A plot of λ_{\max} versus E_{\max} values of UVF2 and UVF3 from A. Colored circles show the average values for UVF2 (blue) and UVF3 (cyan) along with error bars indicating standard deviation. Note that despite overlapping λ_{\max} , the two filters types differ widely in E_{\max} .